A quantum-chemical study of hydride transfer in catalytic transformations of paraffins on zeolites. Pathways through adsorbed nonclassical carbonium ions

V.B. Kazansky [a], M.V. Frash [a,*] and R.A. van Santen [b]

[a] *Zelinsky Institute of Organic Chemistry, Russian Academy of Sciences, Moscow B-334, Russia*
[b] *Eindhoven University of Technology, PO Box 513, Eindhoven, The Netherlands*

Received 14 January 1997; accepted 11 August 1997

A quantum-chemical investigation of the hydride transfer reaction in catalytic transformations of hydrocarbons on zeolites has been performed. Ab initio calculations at the MP2/6-31++G**//HF/6-31G* level demonstrated that the activated complexes of hydride transfer reaction in catalytic transformations of paraffins on zeolites very much resemble adsorbed nonclassical carbonium ions. However, these transient species are strongly held at the surface active sites by the Coulomb interaction. The calculated activation energies for reactions involving propane and isobutane are in a reasonable agreement with the experimental data.

Keywords: activation of alkanes, carbenium ions, carbonium ions, catalytic cracking, hydride transfer, transition states

1. Introduction

Catalytic cracking and skeletal isomerisation of paraffins on solid acids such as zeolites and amorphous silica–alumina are very important processes in the modern refinery. It is generally accepted that these are chain reactions initiated when some carbenium ions have been formed on the catalyst surface [1]. Propagation of the chain includes hydride transfer from an alkane to the adsorbed carbenium ion:

$$R^+_{1\,ads} + R_2{-}H \rightarrow R_1{-}H + R^+_{2\,ads} \qquad (1)$$

Subsequent chemical transformations of the new carbenium ion $R^+_{2\,ads}$ provide an ion with a smaller number of carbon atoms and/or another carbon skeleton:

$$R^+_{2\,ads} \begin{cases} \rightarrow R^+_{3\,ads} + \text{olefin} & \text{(cracking)} \\ \rightarrow R^+_{4\,ads} & \text{(skeletal isomerisation)} \end{cases} \qquad (2)$$

Thus, the hydride transfer reaction is an essential elementary step in the reaction chain.

The direct experimental investigation of hydride transfer in zeolites is difficult, since it is a secondary reaction accompanied by several other processes. However, the activation energies for some hydride transfer reactions have been deduced in ref. [2] from the kinetic modelling of the isobutane cracking. These data together with the regularities observed in ref. [3] indicate that the activation barrier for hydride transfer should be slightly lower than that for protolytic cracking of the corresponding paraffins. An additional source of information concerning hydrocarbon catalytic transformations and in particular their molecular mechanisms has been provided in the last several years by quantum-chemical calculations.

Mechanisms of the reactions (1) and (2) have been traditionally discussed similar to those for free carbenium and carbonium ions or weakly solvated species in super acid solutions. However, adsorbed carbocations are by no means free, but strongly interact with the catalyst surface. Such an interaction influences the structure and chemical properties of these active intermediates.

An investigation of the interaction of adsorbed carbenium ions with the surface of zeolites was only recently achieved by the IR study of proton transfer to the adsorbed molecules [4,5]. These data together with the results of the MAS NMR studies of protonated species [6–8] and of quantum-chemical calculations on the olefin protonation [9–12] show that the ground states of ''adsorbed carbenium ions'' are actually alkoxides covalently bound to the zeolite surface. These species, however, can be relatively easily excited by stretching of carbon–oxygen bonds to carbenium ion-like transition states.

Several recent quantum-chemical studies of hydrocarbon reactions in zeolites were devoted to the H/D exchange with paraffins [13–15] and benzene [16], adsorption of methanol [17–19] and formation of dimethyl ether [20]. Calculations on protolytic cracking and dehydrogenation of paraffins in zeolites [15,21–26] indicated that the adsorbed carbonium ions arising from protonation of paraffins represent high-energy activated complexes or transition states with significantly higher activation barriers of formation than in case of protonation of olefins.

Below we report the results of a quantum-chemical

* To whom correspondence should be addressed.

investigation of the hydride transfer reaction on the zeolite surface between paraffins and the activated carbenium ion-like alkoxides.

2. Models and computational details

All calculations were performed with the GAUSSIAN-92 program [27]. The molecular cluster $H_2OAl(OH)_3$ was used as a model of the zeolite Brønsted acid site. Geometries of the investigated structures were fully optimised at the SCF level with the standard 6-31G* basis set using the gradient technique [28]. Analytical frequency calculations were performed in order to test the nature of the stationary points obtained. The intrinsic reaction coordinate method (IRC) [29] was used for the transition states to determine the reactants and products. Activation energies were calculated at the MP2(FC)/6-31++G**//HF/6-31G** level and corrected for the zero-point energies (ZPE) obtained from the frequency calculations (unscaled frequencies were used). Potential-fitted atomic charges obtained according to the CHELPG scheme [30] at the HF/6-31++G**//HF/6-31G* level were applied for analysis of the charge distribution in the calculated structures.

The effects of the geometry optimisation at the correlated MP2(FU)/6-31G* level and of the usage of the larger $H_3Si(OH)AlH_2OSiH_3$ cluster instead of the smallest $H_2OAl(OH)_3$ one were tested for the systems involved in the methane–methyl transfer. The electron correlation effects are known to be very important for description of the free nonclassical carbocations [31]. This raises a question: are the correlated MP2 final energies computed for the SCF optimised structures sufficient for the reactions involving the adsorbed carbonium ions, or is the correlated geometry optimisation essential. The results given in table 1 indicate that the reaction energy E1 (for formation of the simplest hydride transfer activated complex – ethylcarbonium ion $[CH_3–H–CH_3]^+_{ads}$ – from methane and surface methoxide) is very sensitive to the level of the final energy calculation. However, the effect of the geometry optimisation level on the E1 value is only 2–3 kcal/mol. In particular, the MP2/6-31++G**//MP2/6-31G* (MP2 optimised geometry) and MP2/6-31++G**//HF/6-31G* (SCF optimised geometry) values differ by 1.6 kcal/mol only. This suggests that the MP2/6-31++G**//HF/6-31G* level provides a reasonable description of the other hydride transfer reactions considered.

The data of table 1 show also that the E1 values found with the $H_3Si(OH)AlH_2OSiH_3$ cluster are lower by 5–9 kcal/mol than those found at the same level of calculations with the smallest $H_2OAl(OH)_3$ cluster. This might be caused by the differences in acid strength of the clusters (see section 3.3).

3. Results

Five examples of the hydride transfer reaction will now be discussed. Hydride transfer between propane and the adsorbed *s*-propyl cation, i.e. secondary–secondary transfer, can be considered as a model of the hydride transfer step in cracking of linear paraffins. Propane–*t*-butyl, i.e. tertiary–secondary transfer, is a model of the hydride transfer step in skeletal isomerisation of paraffins. These two reactions will be compared with isobutane–*t*-butyl transfer (already discussed in our previous paper devoted to the isobutane cracking [25]) and the two model reactions of methane–methyl and ethane–ethyl transfer.

3.1. Adsorbed carbonium ions $[R_1–H–R_2]^+_{ads}$

The hydride transfer reaction starts with an attack of a paraffin on the covalently bound surface alkoxide. This results in stretching and strong polarisation of the C–O bond and formation of the adsorbed nonclassical $[R_1–H–R_2]^+$ carbonium ion. Decomposition of such an activated complex results in abstraction of the new paraffin molecule and formation of the new surface alkoxide:

$$R^+_{1\,ads} + R_2–H \rightarrow [R_1–H–R_2]^+_{ads} \rightarrow R_1–H + R^+_{2\,ads} \quad (1a)$$

Calculated structures of the adsorbed nonclassical carbonium ions $[R_1–H–R_2]^+_{ads}$ are depicted in figures 1–3. For both $[C_2H_5–H–C_2H_5]^+_{ads}$ and $[s\text{-}C_3H_7–H–s\text{-}C_3H_7]^+_{ads}$, two energy minima of C_2 symmetry were found. Below only those with the lowest total energies are discussed and depicted in figures 2a and 2b. For

Table 1
Sensitivity of the energy of formation of $[CH_3–H–CH_3]^+_{ads}$ (E1 in figure 1, in kcal/mol) to the level of calculations and to the model cluster

Cluster	Level of the geometry optimisation	Level of the single point calculation			
		HF /6-31G*	MP2(FU) /6-31G*	MP2(FC) /6-31++G**	ZPE correction
$H_2OAl(OH)_3$	//HF/3-21G	81.9	73.9	67.9	−0.8
$H_2OAl(OH)_3$	//HF/6-31G*	81.9	74.2	67.3	−0.8
$H_2OAl(OH)_3$	//MP2(FU)/6-31G*	84.5	72.2	65.7	+0.1
$H_3Si(OH)AlH_2OSiH_3$	//HF/6-31G*	72.7	66.2	61.9	−0.6

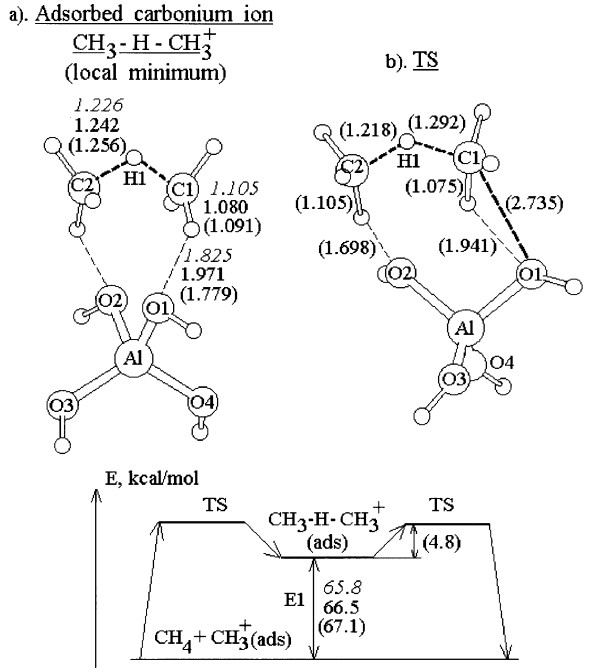

Figure 1. (a) Adsorbed carbonium ion $[CH_3–H–CH_3]^+_{ads}$ (local minimum). (b) Transition state for its decomposition (imaginary frequency 314 cm^{-1}). Distances (in Å): italic figures – MP2/6-31G*; straight figures – HF/6-31G*; figures in parentheses – HF/3-21G. Energies (in kcal/mol): italic figures – MP2/6-31++G**//MP2/6-31G*; straight figures – MP2/6-31++G**//HF/6-31G*; figures in parentheses – MP2/6-31++G**//HF/3-21G.

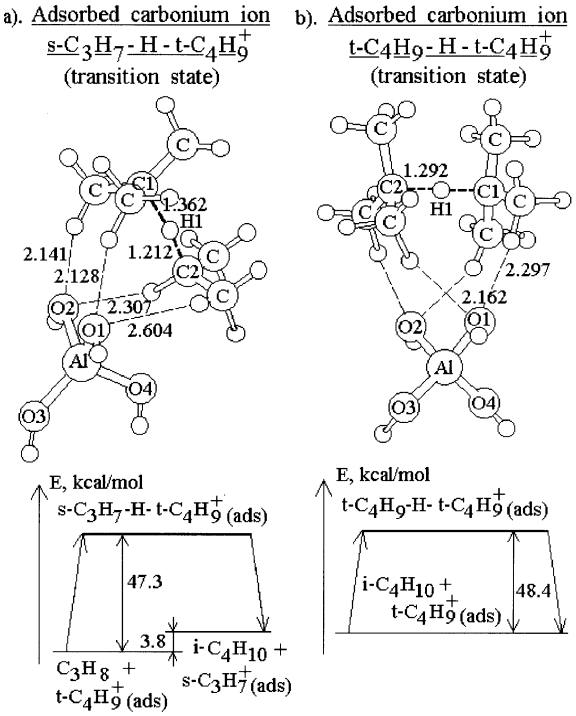

Figure 3. (a) Adsorbed carbonium ion $[s\text{-}C_3H_7–H–t\text{-}C_4H_9]^+_{ads}$ (transition state, imaginary frequency 268 cm^{-1}). (b) Adsorbed carbonium ion $[t\text{-}C_4H_9–H–t\text{-}C_4H_9]^+_{ads}$ (transition state, imaginary frequency 423 cm^{-1}). Distances (in Å) calculated at the HF/6-31G* level, energies (in kcal/mol) – at the MP2/6-31++G**//HF/6-31G* level.

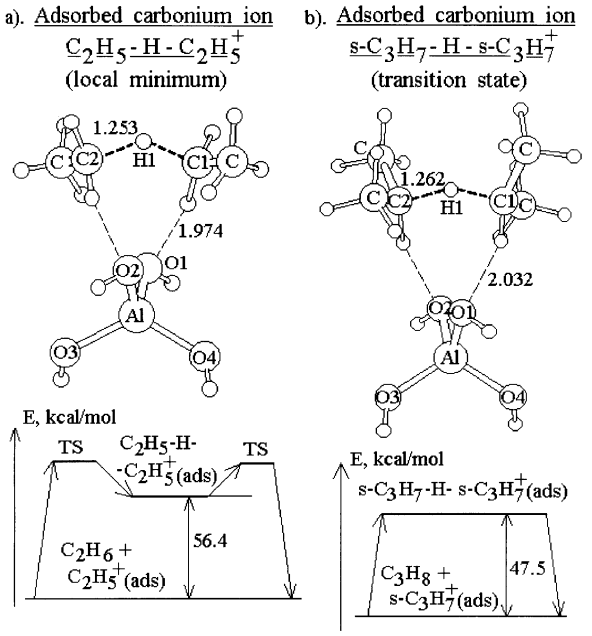

Figure 2. (a) Adsorbed carbonium ion $[C_2H_5–H–C_2H_5]^+_{ads}$ (local minimum). (b) Adsorbed carbonium ion $[s\text{-}C_3H_7–H–s\text{-}C_3H_7]^+_{ads}$ (transition state, imaginary frequency 60 cm^{-1}). Distances (in Å) calculated at the HF/6-31G* level, energies (in kcal/mol) – at the MP2/6-31++G**//HF/6-31G* level.

$[CH_3–H–CH_3]^+_{ads}$ (figure 1) as well as for $[t\text{-}C_4H_9–H–t\text{-}C_4H_9]^+_{ads}$ (figure 3b) only a single minimum energy conformation was found. For $[s\text{-}C_3H_7–H–t\text{-}C_4H_9]^+_{ads}$, the conformation depicted in figure 3a was obtained by substitution of one $s\text{-}C_3H_7$ group in $[s\text{-}C_3H_7–H–s\text{-}C_3H_7]^+_{ads}$ by the $t\text{-}C_4H_9$ group.

The geometry and charge distribution in the hydrocarbon fragments of all the activated complexes (see figures 1–3 and table 2) very much resemble those in nonclassical carbonium ions. Indeed, the high positive charges of these species (about +0.9 *e*) are mainly divided between both alkyl fragments R_1 and R_2. These two fragments are connected by the central hydrogen atom with only small positive or even negative charge. The "hydride" nature of this hydrogen follows from its charge and from the fact that the central C–H bonds (1.212–1.292 Å) are longer than normal C–H bonds in alkanes. An increase of the number of CH_3-substitutions at the central carbon atoms in $[R–H–R]^+_{ads}$ results in an increase of the C1–H1–C2 angle (from 119.2° for $[CH_3–H–CH_3]^+_{ads}$ up to 179.8° for $[t\text{-}C_4H_9–H–t\text{-}C_4H_9]^+_{ads}$) and in an increase in the positive charges on R fragments. This is not surprising, because the higher positive charges on fragments R reflect the higher stability of these carbenium ion-like fragments, whereas the larger C1–H1–C2 angles indicate the more "hydride" character of the central hydrogens.

Table 2
Geometry and charge parameters (distances in ångstroms, angles in degrees, charges in multiples of the electron charge) of the activated complexes $[R1–H–R2]^+_{ads}$, activation energies $E^{\#}$ for the corresponding hydride transfer reactions and energies of the ion pair separation E_{sep} from the activated complexes (in kcal/mol, calculated at the MP2/6-31++G**//HF/6-31G* level with the ZPE corrections)

R1	CH_3	C_2H_5	s-C_3H_7	t-C_4H_9	t-C_4H_9
R2	CH_3	C_2H_5	s-C_3H_7	s-C_3H_7	t-C_4H_9
∠(O1AlO2) (C1AlC2)	89.7	75.0	75.5	82.2	68.8
∠C1–H1–C2	119.2	137.0	156.0	170.4	179.8
Q(R1)	+0.413	+0.408	+0.458	+0.642	+0.572
Q(R2)	+0.413	+0.408	+0.458	+0.476	+0.572
Q(H1)	+0.097	+0.054	+0.003	−0.145	−0.146
Q([R1–H1–R2])	+0.923	+0.870	+0.919	+0.973	+0.998
$E^{\#}$	66.6	56.4	47.5	$E^{\#}_{fwd} = 47.3$ $E^{\#}_{rev} = 43.5$	48.4
E_{sep}	105.1	100.6	96.7	–	85.4

On the other hand, the adsorbed carbonium ions are by no means free, but strongly interact with the negatively charged zeolite surface. Indeed, the C1 and C2 atoms are situated out of the O1–Al–O2 plane of the cluster (dihedral angles (C1–Al–C2)(O1–Al–O2) change from 89.7° for $[CH_3–H–CH_3]^+_{ads}$ to 68.8° for $[t$-$C_4H_9–H–t$-$C_4H_9]^+_{ads}$). It is likely that such an orientation allows the most efficient Coulomb interaction of the positively charged hydrocarbon fragments with the negatively charged cluster. In addition, in all of these structures hydrogen bonds with oxygen atoms of the zeolite model are formed.

The calculated energies of abstraction of the hydrocarbon portions of the activated complexes as free carbonium ions are also given in table 2. An increase of the number of methyl substitutions at the central C1 and C2 carbon atoms of the $[R_1–H–R_2]^+$ fragment makes this fragment more stable and therefore reduces the ion pair separation energy. However, even the most stable hydrocarbon fragment in the $[t$-$C_4H_9–H–t$-$C_4H_9]^+_{ads}$ complex interacts very strongly with the cluster (ion pair separation energy is 85 kcal/mol). Similar large ion pair separation energies (85–89 kcal/mol) have been found in ref. [23] for the activated complexes of the protolytic cracking of *n*-butane.

3.2. Pathways of the hydride transfer reactions

Now we describe the pathways for the formation of the above discussed adsorbed carbonium ions from (and their decomposition to) the corresponding surface alkoxides and paraffins.

Calculated vibration frequencies show that the $[s$-$C_3H_7–H–s$-$C_3H_7]^+_{ads}$, $[s$-$C_3H_7–H–t$-$C_4H_9]^+_{ads}$ and $[t$-$C_4H_9–H–t$-$C_4H_9]^+_{ads}$ complexes represent transition states (all three complexes have one imaginary mode, 60, 268, and 423 cm^{-1} respectively). It was found that the reaction path leads from these transition states to the corresponding surface alkyl groups and free paraffins. Thus, the activation energy of the hydride transfer reaction in all these cases is the difference between the energies of the transition state $[R_1–H–R_2]^+_{ads}$ and the sum of the energies of the surface alkoxides and paraffins.

On the other hand, the $[CH_3–H–CH_3]^+_{ads}$ and $[C_2H_5–H–C_2H_5]^+_{ads}$ complexes of figures 1a and 2a are local minima, since they have no imaginary frequencies. Note that this does not imply that these species could be experimentally detected or studied. Their formation is highly endoergic and therefore the equilibrium concentration of such species should be very low.

We could not find the transition states for decomposition of these activated complexes into surface alkoxides and paraffins at the HF/6-31G* level because the potential energy surfaces are very shallow. A point with one negative vibrational mode and rather small gradients was located on the HF/6-31G* potential energy surface for the $[CH_3–H–CH_3]^+_{ads}$ system; however, it was not possible to reach convergence on gradients and displacements. A transition state for the decomposition of $[CH_3–H–CH_3]^+_{ads}$ into methane and a surface methyl group was, however, found at the HF/3-21G level (see figure 1). This transition state was tested by the IRC method. Thus, the barrier for decomposition of $[CH_3–H–CH_3]^+_{ads}$ was found to be 4.8 kcal/mol at the MP2/6-31++G**//HF/3-21G level with the ZPE corrections. One can assume that for decomposition of $[C_2H_5–H–C_2H_5]^+_{ads}$ the barrier should be even lower, since for the structures with larger number of CH_3 substitutors, $[s$-$C_3H_7–H–s$-$C_3H_7]^+_{ads}$ and $[t$-$C_4H_9–H–t$-$C_4H_9]^+_{ads}$, the barrier does not exist at all. Therefore, as a first approximation, we postulate that the activation energy of methane–methyl and ethane–ethyl hydride transfer is the difference between the energy of $[R_1–H–R_2]^+_{ads}$ and the sum of the energies of the surface alkoxide and paraffin.

3.3. Activation energies

The calculated activation energies for the hydride transfer reactions are collected in table 2. Methane–

methyl transfer has the highest activation barrier (66.5 kcal/mol), and ethane–ethyl transfer the second one (56.4 kcal/mol). This is in agreement with chemical experience, according to which hydride transfer should be much easier from tertiary and secondary carbons than from primary carbons and especially from methane.

In the previously reported DFT calculations [24], the activation energy for hydride transfer from methanol to the surface methyl group was found to be 48.3 kcal/mol. This value is considerably lower than that found in the present work for methane–methyl transfer (66.5 kcal/mol). Such a difference may result from the difference between the methods of calculation used (DFT vs. MP2 and Hartree–Fock). However, it is more likely that the difference in activation energies is due to the difference in the electronic structure of the two transition states. Indeed, in case of hydride transfer from methanol the transition state contains the positively charged CH_2OH fragment. Due to an interaction of the oxygen lone pair electrons with the carbon atom, the CH_2OH fragment is more stable than the CH_3 fragment of the activated complex for methane–methyl transfer, and therefore the transition state in the former case lies lower in the potential energy surface.

The calculated activation energies for propane–*s*-propyl, propane–*t*-butyl, and isobutane–*t*-butyl transfers are very close to each other (47–48 kcal/mol). Thus, substitution of the *s*-C_3H_7 fragment by the *t*-C_4H_9 fragment does not stabilise the transition state for hydride transfer. This is probably a result of steric hindrances for the *t*-C_4H_9 fragment, which causes the larger charge separation in the activated complex.

It was mentioned above that the propane–*s*-propyl hydride transfer is a model of the hydride transfer step in cracking of linear alkanes, while propane–*t*-butyl transfer is a model of such step in skeletal isomerisation. Given the close values of the activation energies for these steps (47.5 and 47.3 kcal/mol), one can conclude that the difference in rates between the cracking and skeletal isomerisation processes is not due to the hydride transfer step involved. Such difference should be caused by the difference in rates between the specific elementary steps, i.e. between cracking and skeletal isomerisation of adsorbed carbenium ions shown in eq. (2).

Now the calculated activation energies will be compared with available experimental data. Hydride transfer is a secondary reaction and direct experimental measurement of its activation energy is difficult. However, it was shown in ref. [3] that the activation barrier for hydride transfer is slightly lower than the barrier of about 40 kcal/mol for protolytic cracking of the corresponding paraffins. The activation energies for hydride transfer from propane to the adsorbed *t*-butyl cation (34.94 kcal/mol) and from methylbutane to the adsorbed *t*-butyl cation (28.03 kcal/mol) were also estimated from the kinetic modelling of isobutane cracking in ref. [2]. Both these values are 12–20 kcal/mol lower than those obtained by us for the $C_3H_8 + s\text{-}C_3H_{7\,ads}^+$, $C_3H_8 + t\text{-}C_4H_{9\,ads}^+$, and $i\text{-}C_4H_{10} + t\text{-}C_4H_{9\,ads}^+$ reactions.

However, the kinetic modelling in ref. [2] implies some rather rough assumptions, for instance, activation energies for several exothermic reactions are set to be zero. In addition, the activation energies of ref. [2] most likely represent the apparent values and therefore should be increased by the adsorption heats of the corresponding paraffins (10–15 kcal/mol).

At the same time, the smallest cluster $H_2OAl(OH)_3$ used in our calculations has a lower acid strength in comparison with real zeolites. Measurements of the O–H stretching frequency shifts upon adsorption of CO [32] led to a deprotonation energy range 266–285 kcal/mol for a number of acidic zeolites (US-Y, HZSM-5, HEMT and HY). Another deprotonation energy range – 284 to 317 kcal/mol – was found for in HZSM-5 in ref. [33]; however, it was argued in ref. [34] that this range should be narrowed to 291–300 kcal/mol. Quantum-chemical calculations with corrections for cluster size, type of functional, and basis set quality [34] gave a deprotonation energy of 295.4 kcal/mol for an ''average'' aluminosilicate.

The deprotonation energy of the $H_2OAl(OH)_3$ cluster is 317.5 kcal/mol (at the MP2/6-31++G**//HF/6-31G* level with ZPE corrections), i.e. significantly larger than the values above. This cluster is electronically too rigid; the negative charge of its anion $Al(OH)_4^-$ is not delocalized enough because of the small cluster size. The deprotonation energy of the larger $H_3Si(OH)Al$ H_2OSiH_3 cluster – 302.3 kcal/mol (at the MP2/6-31++G**//HF/6-31G* level with ZPE corrections) – is closer to the values from refs. [32–34], and the activation energy for the $CH_4 + CH_{3\,ads}^+$ reaction calculated for this cluster is 5.2 kcal/mol lower than for the smallest $H_2OAl(OH)_3$ cluster (see table 1). If larger clusters are used, one can expect a similar decrease in the calculated activation energies for the other hydride transfer reactions.

With respect of all these corrections, the results of our calculations are in a reasonable agreement with the experimental data.

4. Discussion

It is very important to realise that the activation energies for hydride transfer on zeolites (both the above calculated figures and those obtained from the modelling of kinetics in ref. [2]) are very much higher than the activation energies for hydride transfer in liquid super acids (the latter values were collected in ref. [35]). For instance, the activation energy of hydride transfer from the secondary carbon atoms of *n*-hexane and 2,2-dimethylbutane to the tertiary carbenium ions was

reported to be 13–14 kcal/mol [36], whereas the activation energy of hydride transfer from isobutane to the *t*-butyl cation is only 3.6 kcal/mol [37].

This difference is caused by the interaction of hydrocarbon intermediates with the negatively charged zeolite surface in case of hydride transfer in zeolites, instead of solvation of charged species in case of liquid super acids. A diagram of such interaction as it follows from our present calculations together with the data from ref. [25] is shown in figure 4. A ground state of the *t*-butyl fragment is an alkoxide covalently bound to the zeolite model (R(C–O) = 1.5 Å). Stretching of this bond to 2.6 Å simultaneously with transfer of one of *t*-butyl protons towards the neighbouring zeolite oxygen results in the carbenium ion-like transition state for the isobutene formation (see ref. [25]). Alternatively, if the *t*-butyl fragment, instead of splitting off a proton, interacts with a new isobutane molecule, the carbonium ion-like transition state of hydride transfer (figure 3b) is formed. In the latter case, the C–O bond is completely broken – a distance between these atoms is about 3.8 Å, and the activation energy is higher – 48 kcal/mol rather than 36 kcal/mol. However, even in case of the carbonium ion-like transition states, the hydrocarbon fragment is strongly held at the surface by the Coulomb interaction and possibly by hydrogen bonding. The hypothetical abstraction of this fragment as a cation to infinity would require an additional energy of about 85 kcal/mol, which is almost twice as high as the activation energy for the hydride transfer reaction. Such a strong interaction modifies the reactivity of adsorbed species in comparison with free carbocations.

Finally, a possible alternative pathway for the hydride transfer reactions will be discussed. For this, we compare the published quantum-chemical investigation results for another carbonium-ionic reaction in zeolites – protolytic cracking of paraffins. DFT calculations of Collins and O'Malley for *n*-butane cracking [23] and our Hartree–Fock calculations for isobutane cracking [25] predicted similar activation energies for these reactions (52.7–60.8 kcal/mol in ref. [23], 57.5 kcal/mol in ref. [25]) and similar carbonium ion-like transition states with three-centred nonclassical C–H–C bond. However, our calculations [25] indicated formation of methane and surface *s*-propoxide after decomposition of such a transition state (see figure 5a). On the other hand, the calculations of Collins and O'Malley indicated transfer of a hydrogen atom of the carbonium ion to a zeolite oxygen and formation of methane and propene instead of methane and surface alkoxide (see figure 5b).

Such a difference in paths for protolytic cracking can be caused by two reasons. The first is a difference in computational methods. In ref. [25], geometries were optimised at the SCF level, and the SCF method is known to underestimate the strength of hydrogen bonding [38]. However, some DFT methods tend to overestimate this strength [38], and this might make the proton transfer to the zeolite oxygen easier. The second possible reason for the difference in paths is a difference between *n*-butane and isobutane chemistry: a primary alkyl fragment is to be formed in *n*-butane cracking, while the more stable secondary alkyl fragment – in *i*-butane cracking. For ethane protolytic cracking, both Hartree–Fock [21] and DFT [24] calculations predicted formation of methane and surface methoxide, since there are not enough carbon atoms in one ethane molecule for formation of methane and olefin.

Also a pathway for hydride transfer reactions with formation of paraffin and olefin instead of paraffin and surface alkoxide can in principle be possible. Such a pathway would be analogous to that found by Collins and O'Malley in ref. [23] for protolytic cracking. A further investigation is necessary to distinguish between the two pathways for protolytic cracking and hydride transfer on the ground of quantum-chemical arguments. However, some experimental data indicate that the main intermediates of the hydrocarbon transformations are surface alkoxides rather than olefins. Thus, an increase of the *n*-heptane initial cracking rate on metal-free H-ZSM-5 by addition of molecular hydrogen in the feed was found in ref. [39]. This is consistent with the assumption that the decomposition of adsorbed intermediates is a rate determining step that is accelerated by hydride

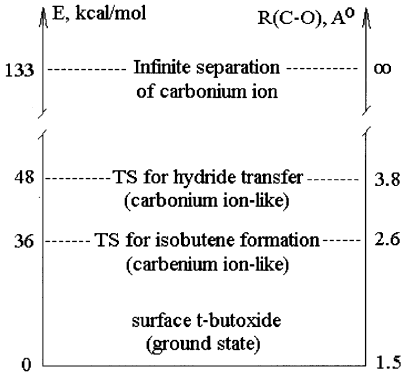

Figure 4. Diagram of the interaction of hydrocarbon fragments with the zeolite surface modelled by the cluster.

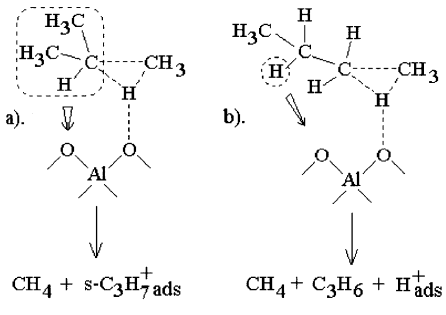

Figure 5. Two pathways found for protolytic cracking of paraffins: (a) for isobutane, Hartree–Fock calculations [25]; (b) for *n*-butane, DFT calculations [23].

transfer from hydrogen. Interpretation of the results [39] is more difficult if the direct formation of olefins during cracking is suggested, because then the active sites are not occupied by alkoxides after cracking step and their regeneration is not required. Consequently, experimental data of ref. [39] agree better with the mechanisms [25] proceeding via formation of surface alkoxides.

5. Conclusion

A quantum-chemical investigation of the hydride transfer reactions in catalytic transformations of paraffins on zeolites has been performed. Calculated activation energies for the propane–*s*-propyl, propane–*t*-butyl, and butane–*t*-butyl transfers are in a reasonable agreement with the available experimental data. The activation energies found for the secondary–secondary and secondary–tertiary hydride transfers are close to each other and suggesting that the difference between cracking and skeletal isomerisation processes is not due to their hydride transfer steps.

The calculations demonstrated that the hydride transfer occurs through adsorbed carbonium ions, which are not relatively stable reaction intermediates, but high-energy activated complexes or transition states. Although the geometry and the charge distribution in such short lived unstable intermediates very much resemble those of free carbocations, these transient species are strongly held at the active sites by a Coulomb interaction. The interaction of the hydrocarbon fragments with the zeolite surface causes much higher activation energies than those earlier reported for hydride transfer in liquid super acids.

Acknowledgement

The authors are grateful to Dr. I.N. Senchenya for helpful discussion on the methodological details. The financial support of Dutch Science Foundation program (NWO) is greatly appreciated.

References

[1] B.W. Wojciechowski and A. Corma, *Catalytic Cracking: Catalysts, Chemistry and Kinetics* (Dekker, New York, 1986).
[2] G. Yaluris, J.E. Rekoske, L.M. Aparicio, R.J. Madon and J.A. Dumesic, J. Catal. 153 (1995) 54.
[3] A. Corma, P.J. Miguel and A.V. Orchilles, J. Catal. 145 (1994) 171.
[4] V.B. Kazansky, Acc. Chem. Res. 24 (1991) 379.
[5] V.B. Kazansky, in: *Advanced Zeolite Science and Technology*, Stud. Surf. Sci. Catal., Vol. 85 (Elsevier, Amsterdam, 1994) p. 251.
[6] M.T. Aronson, R.J. Gorte, W.E. Farneth and D. White, J. Am. Chem. Soc. 111 (1989) 840.
[7] J.F. Haw, B.R. Richardson, I.S. Oshiro, N.D. Lazo and J.A. Speed, J. Am. Chem. Soc. 111 (1989) 2052.
[8] J.F. Haw, J.B. Nicholas, T. Xu, L.W. Beck and D.B. Ferguson, Acc. Chem. Res. 29 (1996) 259.
[9] V.B. Kazansky and I.N. Senchenya, J. Catal. 119 (1989) 108.
[10] I.N. Senchenya and V.B. Kazansky, Catal. Lett. 8 (1991) 317.
[11] P. Viruela-Martin, C.M. Zicovich-Wilson and A. Corma, J. Phys. Chem. 97 (1993) 13713.
[12] E.M. Evleth, E. Kassab, H. Jessri, M. Allavena, L. Montero and L.R. Sierra, J. Phys. Chem. 100 (1996) 11368.
[13] G.J. Kramer, R.A. van Santen, C.A. Emeis and A.K. Nowak, Nature 363 (1993) 529.
[14] R.A. van Santen and G.J. Kramer, Chem. Rev. 95 (1995) 637.
[15] S.R. Blaszkowski, A.P.J. Jansen, M.A.C. Nascimento and R.A. van Santen, J. Phys. Chem. 98 (1994) 12938.
[16] L. W. Beck, T. Xu, J.B. Nicholas and J.F. Haw, J. Am. Chem. Soc. 117 (1995) 11594.
[17] S. Bates and J. Dwyer, J. Chem. Struct. THEOCHEM 112 (1994) 57.
[18] F. Haase and J. Sauer, J. Am. Chem. Soc. 117 (1995) 3780.
[19] R. Shah, J.D. Gale and M.C. Payne, J. Phys. Chem. 100 (1996) 11688.
[20] S.R. Blaszkowski and R.A. van Santen, J. Am. Chem. Soc. 118 (1996) 5152.
[21] V.B. Kazansky, I.N. Senchenya, M.V. Frash and R.A. van Santen, Catal. Lett. 27 (1994) 345.
[22] V.B. Kazansky, M.V. Frash and R.A. van Santen, Catal. Lett. 28 (1994) 211.
[23] S.J. Collins and P.J. O'Malley, Chem. Phys. Lett. 246 (1995) 555.
[24] S.R. Blaszkowski, M.A.C. Nascimento and R.A. van Santen, J. Phys. Chem. 100 (1996) 3463.
[25] V.B. Kazansky, M.V. Frash and R.A. van Santen, Appl. Catal. A 146 (1996) 225.
[26] A.M. Rigby, G.J. Kramer and R.A. van Santen, in press.
[27] GAUSSIAN 92, Revision A, M.J. Frisch, G.W. Trucks, M. Head-Gordon, P.M.W. Gill, M.W. Wong, J.B. Foresman, B.G. Johnson, H.B. Schlegel, M.A. Robb, E.S. Replogle, R. Gomperts, J.L. Andres, K. Raghavachari, J.S. Bincley, C. Gonzalez, R.L. Martin, D.J. Fox, D.J. Defrees, J. Baker, J.J.P. Stewart and J.A. Pople (Gaussian, Inc., Pittsburgh, 1992).
[28] H.B. Schlegel, J. Comp. Chem. 6 (1982) 163.
[29] C.M. Breneman and K.B. Wiberg, J. Comp. Chem. 11 (1990) 361.
[30] C. Gonzalez and H.B. Schlegel, J. Chem. Phys. 90 (1989) 2154.
[31] W.J. Hehre, L. Radom, P.v.R. Schleyer and J.A. Pople, *Ab Initio Molecular Orbital Theory* (Wiley, New York, 1986).
[32] M.A. Makarova, Kh.M. Al-Ghefaili and J. Dwyer, J. Chem. Soc. Faraday Trans. 90 (1994) 383.
[33] J. Datka, M. Boczar and P. Rymarowicz, J. Catal. 114 (1998) 368.
[34] H.V. Brand, L.A. Curtiss and L.E. Iton, J. Phys. Chem. 97 (1993) 12773.
[35] D.M. Brouwer and H. Hogeveen, Progr. Phys. Org. Chem. 9 (1972) 179.
[36] D.M. Brouwer and J.M. Oelderic, Rec. Trav. Chim. 87 (1968) 721.
[37] S. Brownstein and J. Bornais, Can. J. Chem. 49 (1971) 7.
[38] J. Sauer, P. Ugliengo, E. Garrone and V.R. Saunders, Chem. Rev. 94 (1994) 2095.
[39] J. Meusinger and A. Corma, J. Catal. 152 (1995) 189.